TISSUE ENGINEERING: Part A
Volume 21, Numbers 5 and 6, 2015

DOI: 10.1089/ten.tea.2014.0165

Evaluation of Small Intestine Submucosa and Poly(caprolactone-*co*-lactide) Conduits for Peripheral Nerve Regeneration

Sun Woo Shim, MS,[1,*] Doo Yeon Kwon, MS,[1,*] Bit Na Lee, MS,[1,*] Jin Seon Kwon, MS,[1] Ji Hoon Park, MS,[1] Jun Hee Lee, PhD,[2] Jae Ho Kim, PhD,[1] Il Woo Lee, MD, PhD,[3] Jung-Woog Shin, PhD,[4] Hai Bang Lee, PhD,[1] Wan-Doo Kim, PhD,[2] and Moon Suk Kim, PhD[1]

The present study employed nerve guidance conduits (NGCs) only, which were made of small intestine submucosa (SIS) and poly(caprolactone-*co*-lactide) (PCLA) to promote nerve regeneration in a peripheral nerve injury (PNI) model with nerve defects of 15 mm. The SIS- and PCLA-NGCs were easily prepared by rolling of a SIS sheet and a bioplotter using PCLA, respectively. The prepared SIS- and PCLA-NGCs fulfilled the general requirement for use as artificial peripheral NGCs such as easy fabrication, reproducibility for mass production, suturability, sterilizability, wettability, and proper mechanical properties to resist collapsing when applied to *in vivo* implantation. The SIS- and PCLA-NGCs appeared to be well integrated into the host sciatic nerve without causing dislocations and serious inflammation. All NGCs stably maintained their NGC shape for 8 weeks without collapsing, which matched well with the nerve regeneration rate. Staining of the NGCs in the longitudinal direction showed that the regenerated nerves grew successfully from the SIS- and PCLA-NGCs through the sciatic nerve-injured gap and connected from the proximal to distal direction along the NGC axis. SIS-NGCs exhibited a higher nerve regeneration rate than PCLA-NGCs. Collectively, our results indicate that SIS- and PCLA-NGCs induced nerve regeneration in a PNI model, a finding that has significant implications in the future with regard to the feasibility of clinical nerve regeneration with SIS- and PCLA-NGCs prepared through an easy fabrication method using promising biomaterials.

Introduction

Peripheral nerve injury (PNI) is induced by various causes such as mechanical accident, anoxia, hypoglycemia, and pathophysiological events.[1] PNI leads to the loss of neuronal functions and integrity as a result of damage to neurons. Compared with central nervous injury, the peripheral nerve is often more permissive to nerve regeneration.[2] In case of relatively short and mild PNI, typically less than 5 mm, the regeneration process of the injured nerve starts immediately and nerves can spontaneously regenerate from the injured nerve across and beyond the injury site, whereas for severe PNI, regeneration process requires other therapeutic treatment and takes several months.[3–6]

For PNI, nerve autografts have been considered as one of the best methods for a long time.[7] So far, small nerve defects of around 10 mm could be repaired by implanting nerve autografts at the proximal and distal ends of the injured nerve. However, for larger defects, nerve autografts could cause sometimes loss-of-function at the donor site, limited availability of sufficient nerve sources, and discrepancies in the dimension between donor and injured nerves.[8] Therefore, as an alternative to nerve autografts, artificial peripheral nerve guidance conduits (NGCs) have been made to mimic nerve autografts.[9–14]

Many kinds of artificial peripheral NGCs have been developed by using different biomaterials.[9–18] With the development of various biomaterials and fabrication techniques during the previous decades, NGCs have been greatly improved to satisfy the requirement of easy fabrication, reproducibility or availability for mass production, suturability, sterilizability, along with proper mechanical properties to resist collapsing when applied to *in vivo* implantation and regeneration.[9–14]

In terms of NGC fabrication, biomaterial selection and optimization are also important for an ultimately good nerve regeneration outcome. By far, the most commonly used NGC is the hollow tube form of nondegradable silicone.[19]

[1]Department of Molecular Science and Technology, Ajou University, Suwon, Korea.
[2]Nature-Inspired Mechanical System Team, Korea Institute of Machinery and Materials, Daejeon, Korea.
[3]Department of Neurosurgery, Catholic University of Korea, Daejeon, Korea.
[4]Department of Biomedical Engineering, Inje University, Gimhae, Korea.
*Equal first authors.

Silicone NGC has resulted in nerve regeneration over distances up to 10 mm, but often leads to serious chronic tissue inflammation. In addition, nerve regeneration of large nerve defects more than 10 mm remains a significant clinical challenge.

To circumvent these problems, the biomaterials used for NGCs have been switched from silicone to various extracellular matrices (ECM) or biodegradable polymers.[20–23] Several biodegradable NGCs using collagen, poly(caprolactone-*co*-lactide) (PCLA), etc., have already been approved by the US Food and Drug Administration (FDA) and Conformit Europe (CE) for clinical trial of PNI.[24]

Small intestine submucosa (SIS), derived from the submucosal layer of porcine intestine, is an ECM, which consists of more than 90% of the total collagen content of types I and III collagens and several biological factors. Various SIS-based biomedical products have been developed and commercialized due to its good biocompatibility and non-immunogenic property.[25–31] To our knowledge, however, SIS-based NGCs have received little attention at the early stages of *in vivo* research.[32] Thus, SIS may be considered as a candidate to easily give SIS-NGCs.

Recently, computer-aided bioplotter have been used to produce sophisticated scaffolds with interconnected pore structures in relatively short scaffold fabrication time. Thus, the bioplotter can create a microstructured or porous surface morphology on the NGC inner surface.[33–35] In addition, the bioplotter can use various biodegradable synthetic polymers in the fabrication of NGCs, including PCLA biomaterials approved by the US FDA and CE.[24] To the best of our knowledge, no previous study has examined PCLA-NGCs fabricated by using a bioplotter.

Recently, some groups reported the potential possibility of SIS and PCLA-NGCs to enhance nerve regeneration of PNIs in nerve defects of 10 and 14 mm, respectively.[32,36] The overall aim of the current study is to demonstrate that NGCs prepared from SIS and PCLA without any cells and/or growth factors are highly promising candidates to enhance nerve regeneration of PNIs for nerve defects of 15 mm with significant clinical challenge. The following specific questions were addressed: (1) Can the prepared SIS- and PCLA-NGCs fulfill the general requirement as artificial peripheral NGCs? (2) Can SIS- and PCLA-NGCs be utilized for peripheral nerve regeneration? (3) Can SIS- and PCLA-NGCs result in nerve generation? Resolving these issues in the enhancement of peripheral nerve regeneration will have a significant impact on the feasibility of nerve regeneration by only SIS- and PCLA-NGCs without any biological factors through an easy fabrication method using promising biomaterials.

Experimental Section

Preparation of NGCs

Silicone-NGC. Silicone (J.S Silitech) of an inner diameter of 1.72 ± 0.13 mm and wall thickness of 0.58 ± 0.01 mm was obtained and cut to a length of 19 mm. For the animal study, the prepared silicone-NGC was sterilized with ethylene oxide (EO) gas.

Small intestine submucosa–nerve guidance conduit. The preparation procedure for SIS-NGCs was as follows: Sections of porcine jejunum were harvested from market pigs (Woomi Food Company, Finish pig, F_1; Land race + Yorkshire, around 100 kg, 6 months of age, within 4 h of sacrifice). To separate SIS of the porcine jejunum, fat was first removed from the porcine jejunum, followed by carefully washing with water. The porcine jejunum was cut to pieces of ~ 10 cm length and then washed with saline solution. SIS was obtained by complete removal of the tunica serosa and tunica muscularis using scraping with an edge of a Petri dish.[25–30,36] The obtained SIS was washed again with saline solution. The SIS was prepared by cutting in the longitudinal direction, followed by freeze drying using a freeze dryer (Model FDU-540; EYELA) at -80°C for 48 h to give native SIS sheets.

The SIS sheet was put on a stainless steel rod of an outer diameter of 1.6 mm as double layer to fabricate a SIS tube and attached to the wound-up part of the rolled SIS sheet using deionized water (DW). Then, the outer SIS-NGC was slid out from the stainless steel rod. The SIS-NGCs had an inner diameter of 1.68 ± 0.09 mm, a wall thickness of 0.57 ± 0.02 mm, and a length of 19 mm. For the animal study, the prepared SIS-NGCs were sterilized by using EO gas.

Poly(caprolactone-co-lactide)–nerve guidance conduit. For the synthesis of PCLA, all glasses were dried by heating in a vacuum and were handled under a dry nitrogen stream. The typical polymerization process to produce PCLA with a CL/LA ratio of 50/50 (MCL-500) is as follows: MPEG (M_n = 750 g/mol, 0.012 g, 0.016 mmol) as initiator and toluene (80 mL) were introduced into a flask. Water was removed from the MPEG solution by azeotropic distillation before the toluene was distilled off to give a final volume of 30 mL. CL (3.53 g, 30 mmol) and LA (4.46 g, 30 mmol) were added to the MPEG solution at room temperature under a nitrogen atmosphere, followed by the addition of 0.19 mL of a 0.1 M solution of $Sn(Oct)_2$ in dried toluene. After stirring at 130°C for 24 h, the reaction mixture was poured into a mixture of *n*-hexane and ethyl ether (v/v = 4/1) to precipitate PCLA, which was separated from the supernatant by decantation, redissolved in CH_2Cl_2, and then filtered. The resulting solution was concentrated by rotary evaporation and dried in a vacuum to yield a colorless polymer at 96%. The molecular weight of the PCL and PLLA segments in the diblock copolymers were determined as MPEG (750 g/mol)-PCL/PLLA (235,000/265,000 g/mol) from ^{1}H NMR spectra by comparing the intensity of the terminal methoxy proton signal of MPEG at $\delta = 3.38$ ppm, the methylene proton signal of PCL at $\delta = 2.31$ ppm, and the methylene proton signals of PLLA at $\delta = 5.15$ ppm.

The bioplotter was designed and manufactured by Protek. The bioplotting system consisted of a heating jacket and a stainless steel cylinder with a micronozzle (internal diameter 200 μm) to move in the direction of the x–y–z stage by using an air dispenser. The bioplotting system was controlled by a computer software (Tube Scaffold Path Generation SW; Korea Institute of Machinery and Materials), which regulated the pressure, feeding speed, and polymer melting temperature to fabricate the predesigned NGC. PCLA was added to the stainless steel cylinder at 180°C using the heating jacket. When PCLA was melted, a constant air pressure of 50 kPa was applied to the dispenser and a

bioplotted PCLA-NGC was plotted layer-by-layer on a stainless steel duct (1.7 mm outer diameter). The PCLA-NGC pattern was designed with an orthogonal orientation in the layer-to-layer direction with pores of 100 μm in the vertical cross-section. The PCLA was deposited into a series of parallel lines along the Y direction in the first layer, while paralleling to the X direction in the second layer; followed by a procedure of the same deposition in the third layer and fourth layer. The fabricated PCLA-NGCs had an inner diameter of 1.71 ± 0.01 mm, a wall thickness of 0.59 ± 0.02 mm, and a length of 19 mm. For the animal study, the prepared PCLA-NGCs were sterilized by using EO gas.

NGC characterization

For the experiment of wetting of NGCs, the Trypan Blue solution (0.5%) was dropped on each NGC which filled with agar gel in the lumen at room temperature. The images were observed at a cross section of the NGCs for the permeation on each NGC. The compressive modulus of NGC (30 mm long) was tested using an Instron mechanical tester (H5K-T UTM; Tinius Olsen). The load was applied parallel to the perpendicular axis of the NGC. The value of the compressive modulus was determined with a 50% compression of the NGC.

Surgical procedures for NGC implantation

All animals were treated in accordance with the Institutional Animal Experiment Committee at the Ajou University School of Medicine. Sprague Dawley female rats (320–350 g, 10 weeks old) were housed in sterilized cages with sterile food and water and filtered air and handled in a laminar flow hood using aseptic techniques. Rats were anesthetized using Zoletil® and Rompun® (1:1 ratio, 1.5 mL/kg). As shown in Figure 1, the skin and muscle were opened on the mid-thigh of the left side, and microsurgical scissors were used to remove a 15-mm segment of the sciatic nerve. Each NGC of 19 mm length was interposed between the proximal and distal stumps immediately following surgery and then sewed with sutures at 2 mm of each junction. Rats were divided into three experimental groups: Silicone-, SIS-, and PCLA-NGC-implanted groups. All animals survived after this surgical procedure. After implantation of NGCs, the musculature and the skin were sutured. The rats were then allowed to recover in a clean cage on a 37°C heating pad. Antibiotics (gentamicin, 100 μg/kg, i.m.) were given daily for 7 days postinjury.

Surgical procedures for NGC removal and histological evaluation

On weeks 2, 4, 8, and 16 after implantation, rats were sacrificed and individually dissected on the mid-thigh of the left side. The NGC implants with the regenerated nerve inside were carefully removed at the dissected site. The removed NGC implants were observed with the naked eye.

For the histological analysis, the removed NGCs were immediately fixed with 10% formalin for 72 h, dehydrated and embedded in paraffin. The embedded specimens were sectioned (4 μm) along the longitudinal or cross-sectional axis of the implant. Before any staining procedures, paraffin sections were cleared with xylene, and rehydrated through a gradual decrease of ethanol (100%, 95%, 70%, and 60% each), and washed with DW. The sections were then stained with Hematoxylin and Eosin (H&E) or Toluidine blue (Sigma) for 10 min and then washed with DW. After hydration with 95% and 100% alcohol for 5 min each, the

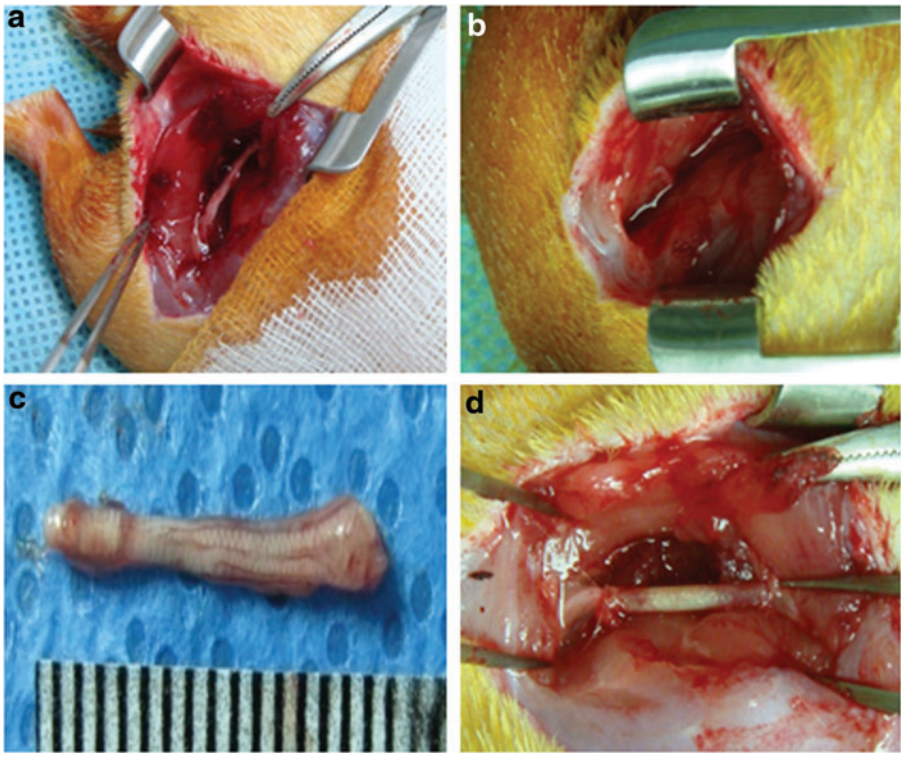

FIG. 1. Optical images of **(a)** sciatic nerve on the left side, **(b)** removal surgery of the sciatic nerve, **(c)** the removed sciatic nerve, and **(d)** implantation of the NGC. NGC, nerve guidance conduit. Color images available online at www.liebertpub.com/tea

sections were cover slipped with water-soluble mount medium (Muto pure chemicals). Toluidine blue-stained images in NGCs indicated myelinated axons.

For the immunohistological analysis, the sectioned specimens were dehydrated in a graded ethanol series, followed by incubation in citrate buffer solution at 120–130°C for 10 min. The slides were washed with phosphate buffered saline (PBS) and PBS-T (0.05% Tween 20 in PBS), blocked with 5% bovine serum albumin (Bovogen) and 5% horse serum (Gibco) in PBS for 90 min at 37°C. The sections were incubated for 16 h at 4°C with a neurofilament (NF) antibody (Cat. ab24706; Abcam) in primary antibody diluent (1:1000; DAKO) and S100A1 antibody for Schwann cells (produced in rabbit, Cat. SAB4502708; Sigma-Aldrich) in antibody diluent (1:1000; DAKO), washed with PBS and PBS-T, and then incubated with the secondary antibody (goat anti-mouse Alexa Fluor®594, Cat. A11005, Invitrogen; donkey anti-rabbit Alexa Fluor594, Cat. A21207, Invitrogen) (1:1000) for 3 h at room temperature in the dark (NF antibody [anti-200 kDa + 160 kDa] in this work can be expressed at all three major NF subunits: NF-L, NF-M, and NF-H). The slides were washed again with DW, counterstained with DAPI (Cat. D9542; Sigma-Aldrich), and then mounted with fluorescent mounting solution (DAKO). Immunofluorescent images were visualized using the Axio Imager A1 (Carl Zeiss Microimaging GmbH) and analyzed with the Axiovision Rel. 4.8 software (Carl Zeiss Microimaging GmbH).

NF-positive cells, S100-positive cells, and DAPI-stained cells indicated axons, Schwann cells, and live cells on NGCs, respectively. NF-positive cells (red), S100-positive cells (red), and DAPI-stained cells (blue) were counted in cross-sectioned images of all NGCs at 2, 4, 8, and 16 weeks. For comparison, NF-positive cells, S100-positive cells, and DAPI-stained cells were individually counted in cross-sectioned images of sciatic nerve removed from normal rats (Supplementary Fig. S1; Supplementary Data are available online at www.liebertpub.com/tea). The percentage of individually counted NF- or S100-positive cells was determined by dividing each mean of the counted NF- or S100-positive cells on the injured sciatic nerve with each NGC by each mean of the counted NF- or S100-positive cells on normal sciatic nerve.

Statistical analysis

Counting of NF- or S100-positive cells was carried out in four rats of independent experiments for each of the four NGC rats. All data are presented as mean and standard deviation. The results were analyzed with one-way analysis of variance with Bonferroni's multiple comparisons, using the SPSS program (version 12.0; SPSS, Inc.).

Results

Preparation and characterizations of NGCs

The images of all NGCs are shown in Figure 2. SIS- and PCLA-NGCs were easily prepared by rolling of a SIS sheet and bioplotter, indicating easy fabrication. The inner diameters and wall thickness of all NGCs showed almost uniform size at every time, indicating reproducibility. There was no change in the original shape of the SIS- and PCLA-NGCs before and after EO sterilization, indicating sterilizability.

All NGCs showed flexible properties as shown in the second column of Figure 2. The silicone-NGC exhibited uniform but smooth close surface morphology and, thus, could not exchange nutrients between the inside and outside of the silicone-NGC. Meanwhile, the SIS-NGC exhibited rough and interconnected fiber surface structures (Supplementary Fig. S2), which may allow exchange of nutrients between the inside and outside of the SIS-NGC. PCLA-NGCs fabricated by using a bioplotter exhibited pores among each layer strand through the layer-by-layer strand (Supplementary Fig. S3). Nutrients can effectively permeate through the pores between the inside and outside of PCLA-NGCs.

Wetting of NGCs using a Trypan Blue solution was performed to examine the permeation of nutrients from the outside to the inside of NGCs as shown in the right side of Figure 2. SIS- and PCLA-NGCs showed rapid permeation of the Trypan Blue solution (3–4 min) through the NGC wall as

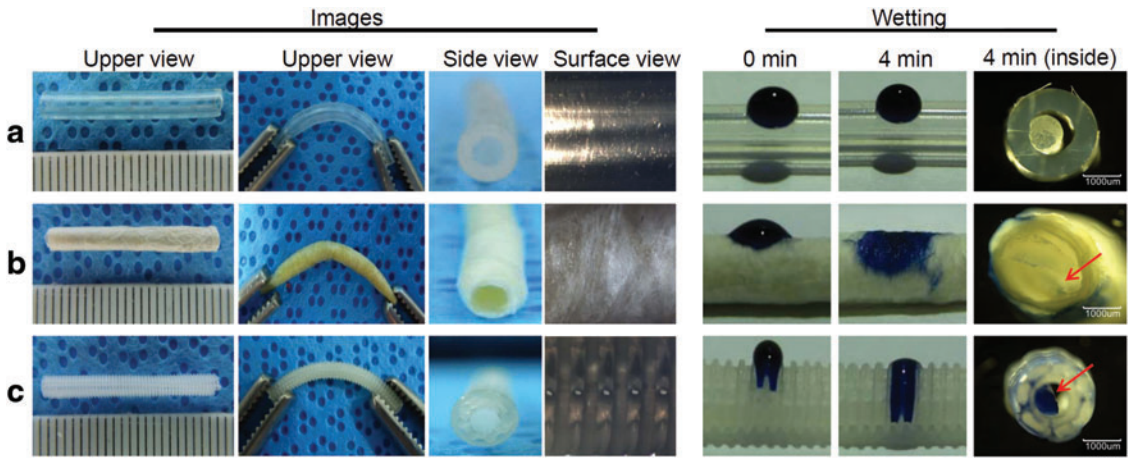

FIG. 2. *Left:* Upper, side, and surface view images and *right:* wetting images at 0 and 4 min of **(a)** silicone NGC, **(b)** SIS-NGC, and **(c)** PCLA-NGC. The arrows indicate the permeated Trypan Blue solution. PCLA, poly(caprolactone-co-lactide); SIS, small intestine submucosa. Color images available online at www.liebertpub.com/tea

shown in cross-section images, indicating their hydrophilic character. Meanwhile, the Trypan Blue solution did not permeate at all through the silicone-NGC.

The compressive modulus of the NGCs was measured to compare maintenance of the structure and resistance to collapse for five specimens. At a 50% compressive ratio, the compressive modulus of the silicone-NGC was measured to be 1.6 ± 0.2 N, which is similar to that of PLGA-NGC of 1.9 ± 0.1 N. The compressive modulus of the SIS-NGC was measured to be 0.4 ± 0.1 N. The tensile modulus of the SIS- had the highest value (156 MPa), while the silicone-NGC had the lowest (3 MPa). The PCLA-NGC exhibited an elastic modulus in-between these two values (17 MPa). Fast nutrient permeation and unique mechanical properties of SIS- and PCLA-NGCs are expected to be very helpful for nerve regeneration.

Functional movement

NGC implantation surgery was well tolerated in all NGC models. After surgery, all animals remained in good health condition and did not show any inflammatory signs or adverse tissue reactions on the mid-thigh of the left side.

All animals seldom moved their left hind legs immediately after surgery. At 2 weeks after implantation surgery, animals of the SIS- and PCLA-NGC groups showed normal movement of the operated left leg and supported their body weight on their hind leg, whereas animals of the silicone-NGC group exhibited slightly awkward movement on the left leg even at 4 weeks after surgery, but showed normal movement thereafter (Supplementary Fig. S4).

NGC after animal surgery

Nerve regeneration was visually analyzed at 2, 4, 8, and 16 weeks postimplant (Fig. 3). Animals of the silicone-NGC group exhibited serious inflammation and formation of a fibrotic capsule inside the NGC, in addition to no apparent neuroma formation during all experimental periods.

SIS- and PCLA-NGCs appeared well integrated into the host sciatic nerve without causing dislocations. In the SIS-NGC group, NGCs were filled with abundant regenerated nerves and surrounded by a thin layer of fibrous tissue on the outside. There was no serious inflammation. Nerve filling occurred from the proximal to the distal end, indicating the presence of nerve regeneration at the injured gap. The junction areas between the SIS-NGC and normal sciatic nerve became already blurry at 2 weeks after surgery due to nerve regeneration into the SIS-NGC. The number of regenerated nerves in SIS-NGCs increased as the implantation time increased. A thin layer of SIS debris was confirmed on the surface of implanted SIS-NGCs at 4 weeks after surgery, but the SIS-NGCs were almost completely degraded at 8 weeks.

PCLA-NGCs exhibited a small quantity of regenerated nerves around the junction areas at 2 weeks after surgery. At 4 weeks, abundant nerves were regenerated inside the NGC. The regenerated nerves grew into the PCLA-NGCs as the implantation time increased from 2 to 16 weeks. Animals in the PCLA-NGC group also exhibited no serious inflammation. The nondegraded PCLA confirmed on surface of implanted PCLA-NGC at 8 weeks.

SIS- and PCLA-NGCs maintained their NGC shape for 8 weeks without collapse, which is an important factor in nerve regeneration. Both SIS- and PCLA-NGCs exhibited remarkable formation of regenerated tissue in proximal junction areas and then gradually grew in the distal direction along the NGC axis.

Histological evaluation of nerve regeneration

Nerve regeneration was evaluated by sectioning in the longitudinal direction through the NGCs and H&E (Fig. 4), Toluidine blue (Fig. 5), NF (Fig. 6), and S100 (Fig. 7) staining to identify nerve regeneration. H&E, Toluidine blue, NF, and S100 staining of normal sciatic nerves

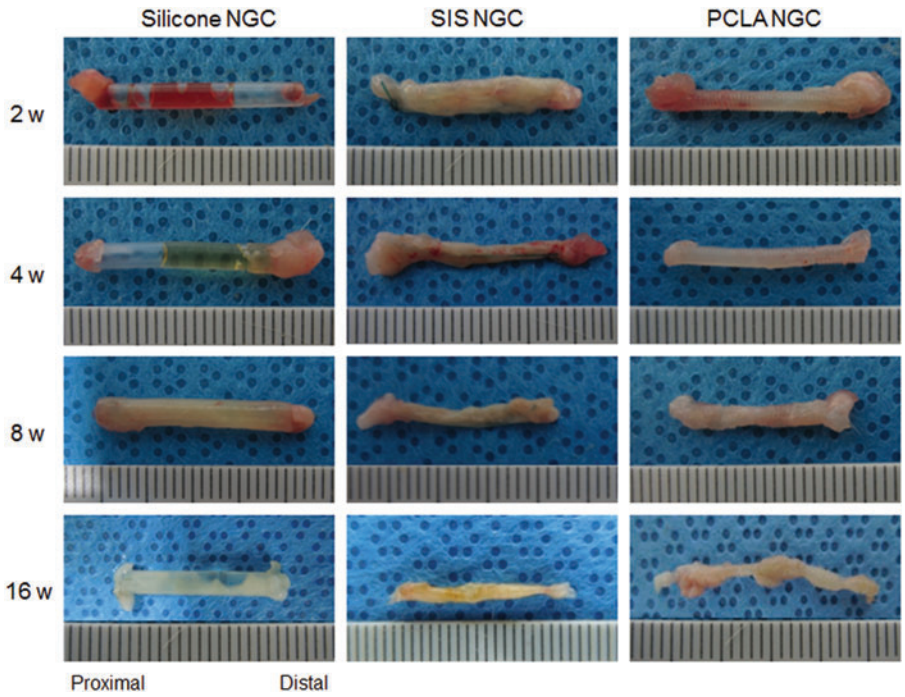

FIG. 3. Images of the removed NGCs at 2–16 weeks after *in vivo* implantation. Color images available online at www.liebertpub.com/tea

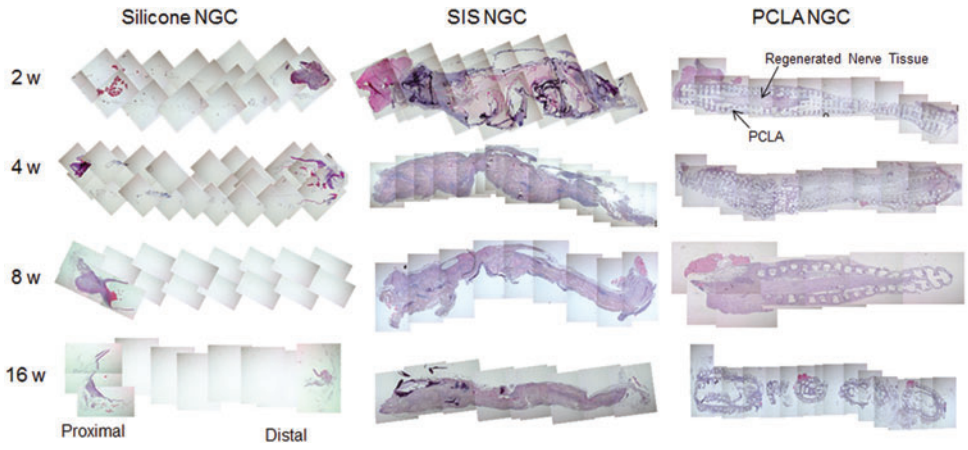

FIG. 4. Hematoxylin and eosin staining of NGCs at 2–16 weeks after *in vivo* implantation. Color images available online at www.liebertpub.com/tea

presented morphologies of regular nerve alignment and sparse oval Schwann cell nuclei among the nerves.

As demonstrated by the results shown in Figure 4, nerve regeneration in H&E staining images of animals of the silicone-NGC group was not observed between proximal and distal areas, and even at junction areas, even at 16 weeks after surgery (Supplementary Fig. S5).

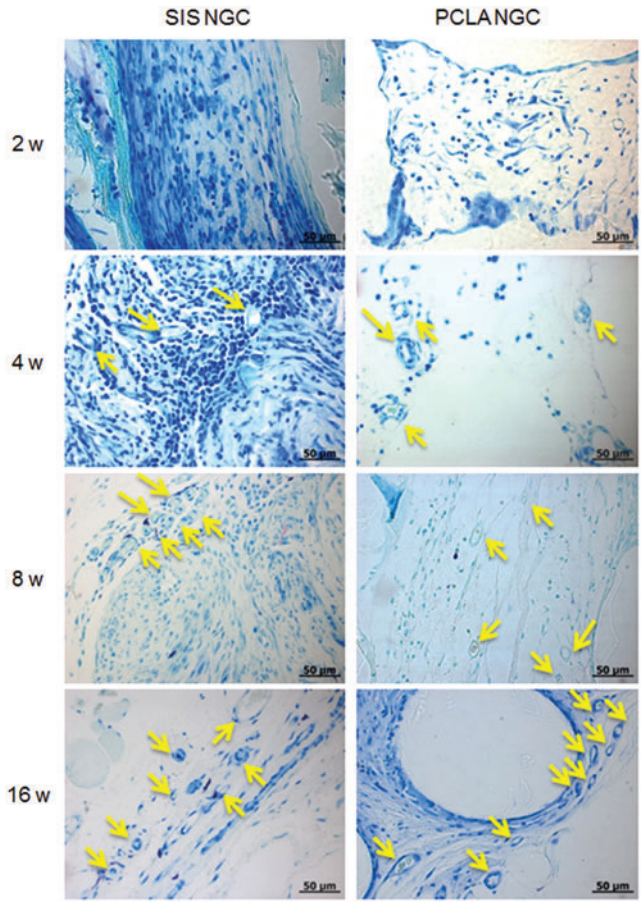

FIG. 5. Toluidine blue staining of NGCs at 2–16 weeks after *in vivo* implantation (Magnification: 400× and scale bars: 50 μm, *yellow arrow*: axon). Color images available online at www.liebertpub.com/tea

Meanwhile, regenerated nerves were observed in H&E staining images of animals of the SIS-NGC group at 2 weeks postimplantation. SIS-NGCs exhibited growth of regenerated nerves through the injury. The nerves of animals in the SIS-NGC group gradually grew at around the lesion only in the SIS- and PCLA-NGC-implanted groups. Partial regeneration of the nerves was confirmed in the central part of the SIS-NGC at 4 weeks postimplantation and at the distal areas at 8 weeks postimplantation.

H&E staining images of animals in the PCLA-NGC-implanted group exhibited regenerated nerves through the empty center space inside of the PCLA-NGCs, which indicates that PCLA-NGC could provide correct guidance for nerve growth. Regenerated nerves were confirmed in H&E staining images of the central part of the PCLA-NGCs at 8 weeks postimplantation and were more evident at the later time points. PCLA-NGCs maintained their NGC structure for up to 8 weeks, because PCLA did not degrade during this time; the main structure was almost completely degraded at 16 weeks postimplantation.

In Toluidine blue-stained sections (Fig. 5), the injury lesions in the SIS- and PCLA-NGC groups showed clear myelinated axons in the center section (arrows). This finding indicates that nerve regeneration occurred after implantation of SIS- and PCLA-NGCs.

NF and S100 staining can provide the evidence for the presence of axons and Schwann cells (Figs. 6 and 7). In animals of the silicone-NGC group, there were no NF- and S100-positive cells (Supplementary Fig. S6). However, NF and S100 staining of longitudinal sections through the injury site provided clear evidence that axonal and Schwann cell regeneration had occurred at around the lesion only in the SIS- and PCLA-NGC-implanted groups. The bottom images of Figures 6 and 7 show enlarged images of NF (red), S100 (red), and DAPI (blue) immunofluorescent staining of SIS- and PCLA-NGC-implanted animals (Supplementary Figs S7–S10).

NF- and S100-positive cells were counted in the total stained tissue area to determine the extent of nerve regeneration and compared with normal sciatic nerves (Fig. 8). The number of NF-positive cells in the SIS-NGC group increased to 2%, 5%, 14%, and 28% at 2, 4, 8, and 16 weeks postimplantation, respectively, indicating *in vivo* axon formation at the implantation site ($*p < 0.001$). The percentage of NF-

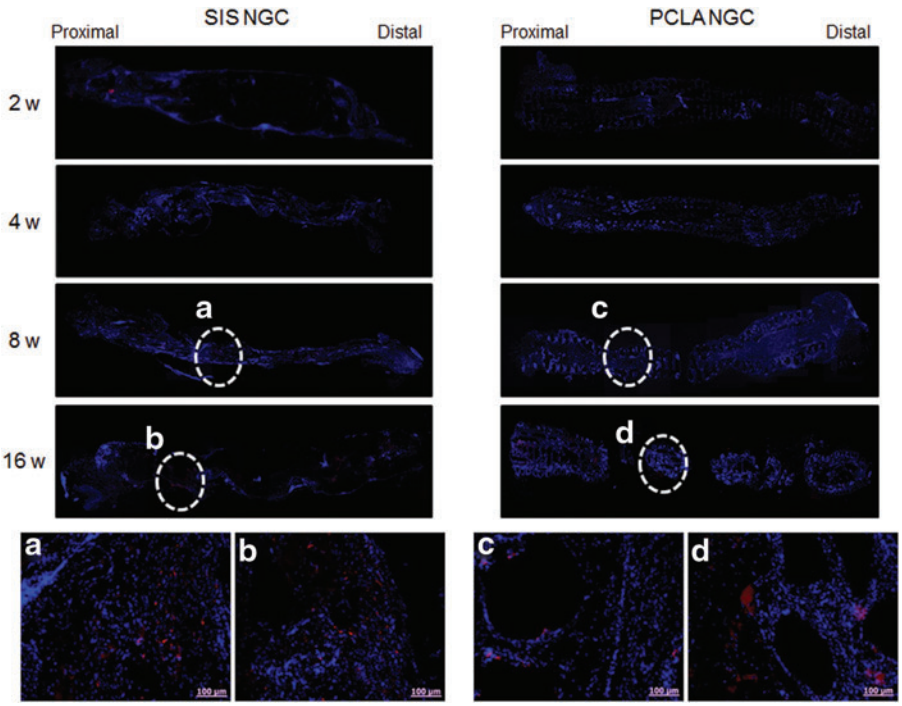

FIG. 6. NF staining (**a–d:** enlarged staining images) of SIS- and PCLA-NGCs at 2–16 weeks after *in vivo* implantation (Magnification: 200× and scale bars: 100 μm). NF, neurofilament. Color images available online at www.liebertpub.com/tea

positive cells in the PCLA-NGC group was below 4% even at 8 weeks and 17% at 16 weeks ($*p < 0.001$). The percentage of S100-positive cells showed a dramatic increase of 54% at 16 weeks in the SIS-NGC group and increased from 1% to 23% between 2 and 16 weeks in the PCLA-NGC group ($*p < 0.001$). There was a statistical observation for an increase in NF- and S100-positive cells with increasing time after surgery ($*p < 0.001$, $**p < 0.01$). The SIS- and PCLA-NGC-implanted animals showed a significant increase in NF- and S100-positive cells compared with silicone-NGC-implanted animals at all experimental time points after PNI.

Discussion

Nerve autografts have by far offered the best results in nerve regeneration.[7] However, as illustrated above, nerve autografts have well-known drawbacks such as donor site loss-of-function, structural differences between donor and recipient grafts, etc.[8] As such, artificial NGCs have been developed over the years. Several groups have reported that artificial NGCs can show comparable or even superior nerve regeneration abilities as compared with nerve autografts.[9–14,37,38] In designing the next generation of NGCs, much consideration has to be

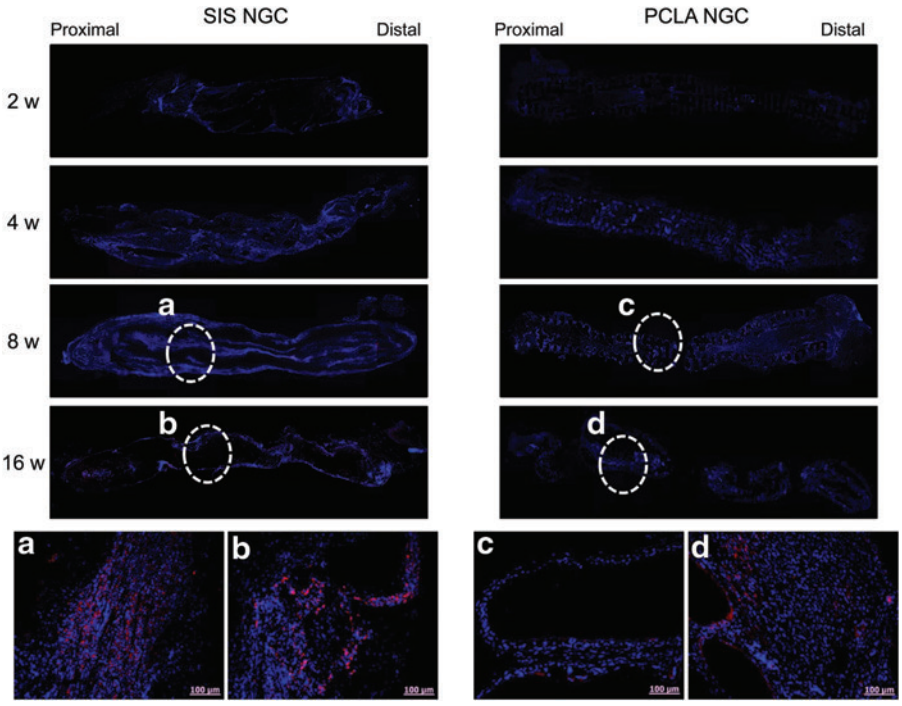

FIG. 7. S100 staining (**a–d:** enlarged staining images) of SIS- and PCLA-NGCs at 2–16 weeks after *in vivo* implantation (Magnification: 200× and scale bars: 100 μm). Color images available online at www.liebertpub.com/tea

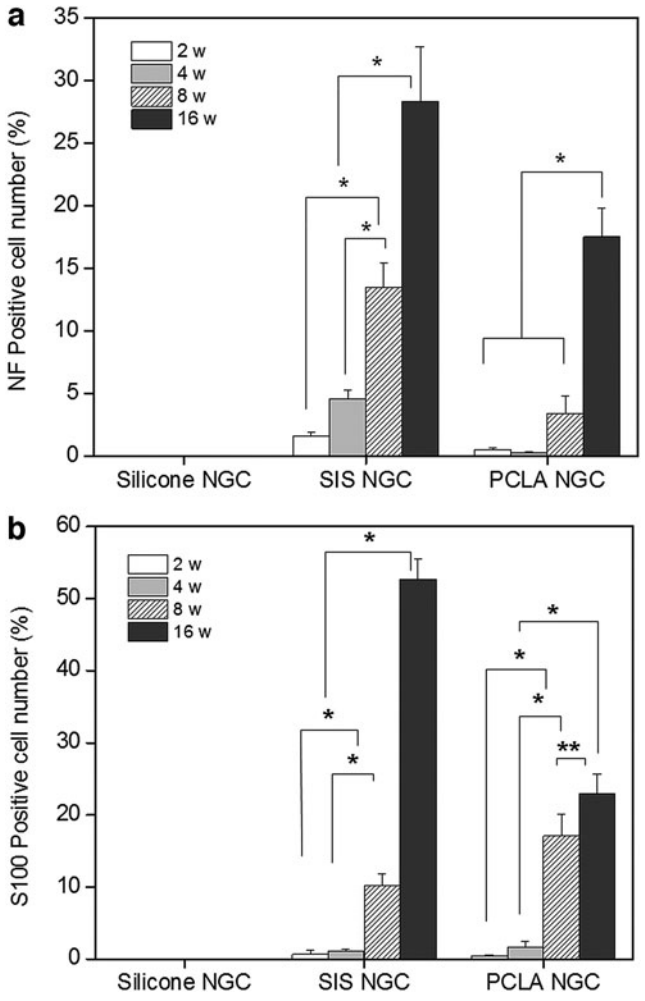

FIG. 8. Numbers of **(a)** NF- and **(b)** S100-positive cells on/in NGCs as a function of time after implantation (*$p < 0.001$, **$p < 0.01$). The percentage of counted NF- or S100-positive cells was determined by dividing each mean of the counted NF- or S100-positive cells on the injured sciatic nerve with each NGC by each mean of the counted NF- or S100-positive cells on normal sciatic nerve.

placed in the selection of an appropriate biomaterial. In addition, little previous study has examined NGCs fabricated by using a simple and versatile fabrication technique. In this study, we selected SIS and PCLA, which gained clinical acceptance as biomaterials for NGC fabrication, in comparison to silicone.

Even though the biological material, which was harvested from another species, affects the host tissue response to material following implantation, it seems apparent that SIS-based biomedical products (SurgiSISs, Cook Biotech, Inc.; Restores, DePuy Orthopaedics, Inc.) are safe for implantation and have received regulatory approval for use in human patients.[24] SIS-NGCs were easily prepared by rolling of an SIS sheet. The preparation process provided reproducible SIS-NGCs with uniform inner sizes. The prepared SIS-NGCs exhibited flexibility and mechanical properties to resist collapsing. SIS-NGCs maintained their original form after EO sterilization.

As another NGC candidate, PCLA-NGCs were easily prepared by using a bioplotter as simple and versatile fabrication technique. The feasibility of PCLA with various proportions of the PLLA and PCL was examined in specific fabrication using a bioplotter. In our result, PLLA/PCL ratio of 50/50 achieved the goal as a biomaterial for fabrication of NGCs with rapid and easy reproducibility using the bioplotter.[39] The prepared PCLA-NGCs exhibited reproducibility of the inner dimensions and feasibility of easy mass production. In addition, the prepared PCLA-NGCs also exhibited flexibility, mechanical properties to resist collapsing, and sterilizability using EO gas. SIS- and PCLA-NGCs possessed better hydrophilicity.

Furthermore, SIS- and PCLA-NGCs exhibited suturability at the proximal and distal ends of the sciatic nerve and were well maintained at the host sciatic nerve without causing dislocations between the proximal and distal ends for the experimental periods. Thus, SIS- and PCLA-NGC prepared in this work greatly satisfied the requirements of easy fabrication, reproducibility for mass production, suturability, and sterilizability along with proper mechanical properties for *in vivo* implantation.

Recently, some groups have investigated the *in vivo* peripheral nerve regeneration at 10-mm sciatic nerve defect gap using SIS and at 14-mm gap using PCLA with nerve growth factor.[32,40] Thus, for *in vivo* peripheral nerve regeneration, we explored the efficacy of SIS- and PCLA-NGCs in bridging a 15-mm sciatic nerve defect gap without any cells and/or nerve growth factors. NGC implantation surgery was well tolerated in all PNI models. Animals in the SIS- and PCLA-NGC groups did not show any inflammation caused by the biomaterials. Animals in the SIS- and PCLA-NGC groups showed normal movement of the operated left legs at 2 weeks; however, the silicone-NGC-implanted PNI animals showed slightly awkward movement at 4 weeks after surgery. Several previous studies have shown that silicone-NGC exhibited slight walking locomotion due to self-recovery of sciatic function.[22,41–44]

The flexibility and mechanical properties of the NGC is an important factor for nerve regeneration to manipulate and resist stretching forces during implant surgery and to retain their shape during the nerve regeneration process.[24–31] Therefore, it is essential to explore the mechanical characteristics of nerve conduits. Our mechanical testing data and animal experiment results showed that the prepared SIS- and PCLA-NGCs had good flexibility and possessed sufficient toughness to resist compression or collapse upon implantation during peripheral nerve regeneration. In the animal implantation experiments, the prepared SIS- and PCLA-NGCs also effectively prevented fibrous tissue infiltration and did not induce damage such as necrosis and inflammation in the surrounding tissue, whereas silicone-NGCs induced severe inflammation.

The degradation rate has also been emphasized as an important factor when considering the design of artificial NGCs because nondegradable silicone would compress regenerated nerves in the long term.[11] SIS-NGCs maintained their original guidance structure for the experimental periods of 8 weeks, which matched well with the nerve regeneration rate. The degradation rate of PCLA-NGCs was also ideally tailored to match the nerve regeneration rate from 2 to 16 weeks. Silicone-NGCs are less desirable because of the nondegradability noted over the observation time of 16 weeks.

We speculate that SIS- and PCLA-NGCs can facilitate axonal outgrowth, which contributes to the necessary sprouting following nerve injury because SIS- and PCLA-NGCs provide sufficient space for spatial guidance of axon and Schwann cell growth. In the present images of H&E staining, all regenerated nerves from the SIS- and PCLA-NGC groups successfully grew through the sciatic nerve-injured gap between the proximal and the distal on the NGC axis. The injured nerves were partially connected at 8 weeks for SIS-NGCs and 16 weeks for PCLA-NGCs.

Nerve regeneration was evaluated by counting NF- and S100-positive cells because they can provide the evidence for the presence of axons and Schwann cells.[45,46] The statistical results indicated that SIS- and PCLA-NGCs resulted in significantly higher numbers of axons and Schwann cells compared with silicone-NGCs at 6 and 12 weeks. In addition, significantly more NF- and S100-positive cells were observed in the SIS-NGC group than in the PCLA-NGC group. The percentage of S100-positive cells of the SIS-NGC group was about 55% of that of normal sciatic nerves. NF- and S100-positive cells were counted in the total stained injured area and the results were compared with those of normal sciatic nerves. Because, in this experiment, we used only NGCs without any cells and/or nerve growth factors, the present findings indicate that SIS- and PCLA-NGCs are promising NGCs for peripheral nerve regeneration at 15-mm sciatic nerve defect gap in the future.

Conclusion

In the present study, the suitability of SIS- and PCLA-NGCs as NGC was examined. The prepared SIS- and PCLA-NGCs fulfilled the general requirement for use as artificial peripheral NGCs such as easy fabrication, reproducibility, suturability, sterilizability, and proper mechanical properties. The *in vivo* evaluation indicated that clinically acceptable SIS- and PCLA-NGCs only, without any biological factors, provide sufficient driving force for guidance of axons and Schwann cells over time. Moreover, the present study shows that the PNI model employing large nerve defects is a valuable tool for testing therapeutic strategies without the confounding effect of any biological factors.

Acknowledgments

This study was supported by a grant from MKE (Grant no. 10038665) and Priority Research Centers Program (2010-0028294) through NRF funded by the Ministry of Education, Science, and Technology.

Disclosure Statement

No competing financial interests exist.

References

1. Iwata, T., Lakshman, S., Singh, A., Yufa, M., Claudio, R., and Hadzić, A. Peripheral nerve blocks for perioperative management of patients having orthopedic surgery or trauma of the lower extremity. Bosn J Basic Med Sci **5,** 5, 2005.
2. Dahlin, L.B. Techniques of peripheral nerve repair. Scand J Surg **97,** 310, 2008.
3. Addas, B.M., and Midha, R. Nerve transfers for severe nerve injury. Neurosurg Clin N Am **20,** 27, 2009.
4. Choi, D., and Raisman, G. Somatotopic organization of the facial nucleus is disrupted after lesioning and regeneration of the facial nerve: the histological representation of synkinesis. Neurosurgery **50,** 355, 2002.
5. Navarro, X., Vivó, M., and Valero-Cabré, A. Neural plasticity after peripheral nerve injury and regeneration. Prog Neurobiol **82,** 163, 2007.
6. Pannucci, C., Myckatyn, T.M., Mackinnon, S.E., and Hayashi, A. End-to-side nerve repair: review of the literature. Restor Neurol Neurosci **25,** 45, 2007.
7. Konofaos, P., and Ver Halen, J.P. Nerve repair by means of tubulization: past, present, future. J Reconstr Microsurg **29,** 149, 2013.
8. Pfister, B.J., Gordon, T., Loverde, J.R., Kochar, A.S., Mackinnon, S.E., and Cullen, D.K. Biomedical engineering strategies for peripheral nerve repair: surgical applications, state of the art, and future challenges. Crit Rev Biomed Eng **39,** 81, 2011.
9. Haastert-Talini, K., Geuna, S., Dahlin, L.B., Meyer, C., Stenberg, L., Freier, T., Heimann, C., Barwig, C., Pinto, L.F., Raimondo, S., Gambarotta, G., Samy, S.R., Sousa, N., Salgado, A.J., Ratzka, A., Wrobel, S., and Grothe, C. Chitosan tubes of varying degrees of acetylation for bridging peripheral nerve defects. Biomaterials **34,** 9886, 2013.
10. Gumera, C., Rauck, B., and Wang, Y. Materials for central nervous system regeneration: bioactive cues. J Mater Chem **21,** 7033, 2011.
11. Angius, D., Wang, H., Spinner, R.J., Gutierrez-Cotto, Y., Yaszemski, M.J., and Windebank, A.J. A systematic review of animal models used to study nerve regeneration in tissue-engineered scaffolds. Biomaterials **33,** 8034, 2012.
12. Yang, X., Jin, Y., Bi, H., Wei, W., Cheng, J., Liu, Z., Shen, Z., Qi, L., and Cao, Y. Peripheral nerve repair with epimysium conduit. Biomaterials **34,** 5606, 2013.
13. Bell, J.H., and Haycock, J.W. Next generation nerve guides: materials, fabrication, growth factors, and cell delivery. Regeneration of completely transected spinal cord using scaffold of Poly(D,L-lactide-co-glycolide)/small intestinal submucosa seeded with rat bone marrow stem cells. Tissue Eng Part B Rev **18,** 116, 2012.
14. Kang, K.N., Kim, D.Y., Yoon, S.M., Lee, J.Y., Lee, B.N., Kwon, J.S., Seo, H.W., Lee, I.W., Shin, H.C., Kim, Y.M., Kim, H.S., Kim, J.H., Min, B.H., Lee, H.B., and Kim, M.S. Tissue engineered regeneration of completely transected spinal cord using human mesenchymal stem cells. Biomaterials **33,** 4828, 2012.
15. Kang, K.N., Lee, J.Y., Kim, D.Y., Lee, B.N., Ahn, H.H., Lee, B., Khang, G., Park, S.R., Min, B.H., Kim, J.H., Lee, H.B., and Kim, M.S. Regeneration of completely transected spinal cord using scaffold of poly(D,L-lactide-co-glycolide)/small intestinal submucosa seeded with rat bone marrow stem cells. Tissue Eng Part A **17,** 2143, 2011.
16. Wong, Y.S., Tay, C.Y., Wen, F., Venkatraman, S., and Lay, T.P. Engineered polymeric biomaterials for tissue engineering. Cur Tissue Eng **1,** 41, 2012.
17. Li, X., Katsanevakis, E., Liu, X., Zhang, N., and Wen, X. Engineering neural stem cell fates with hydrogel design for central nervous system regeneration. Prog Polym Sci **37,** 1105, 2012.
18. Park, S.C., Oh, S.H., and Lee, J.H. Fabrication and characterization of nerve growth factor-immobilized asymmetrically porous PDOCL/Pluronic F127 nerve guide conduit. Tissue Eng Reg Med **8,** 173, 2011.

19. Le Beau, J.M. Growth factor expression in normal and diabetic rats during peripheral nerve regeneration through silicone tubes. Adv Exp Med Biol **321,** 37, 1992.
20. Meek, M.F., and Coert, J.H. US food and drug administration/conformit europe-approved absorbable nerve conduits for clinical repair of peripheral and cranial nerves. Ann Plast Surg **60,** 110, 2008.
21. Volpato, F.Z., Führmann, T., Migliaresi, C., Hutmacher, D.W., and Dalton, P.D. Using extracellular matrix for regenerative medicine in the spinal cord. Biomaterials **34,** 4945, 2013.
22. Cao, J., Xiao, Z., Jin, W., Chen, B., Meng, D., Ding, W., Hou, S.X., Zhu, T., Yuan, B., Wang, J., Liang, W., and Dai, J. Induction of rat facial nerve regeneration by functional collagen scaffolds. Biomaterials **34,** 1302, 2013.
23. Wang, T.Y., Forsythe, J.S., Parish, C.L., and Nisbet, D.R. Biofunctionalisation of polymeric scaffolds for neural tissue engineering. J Biomater Appl **27,** 369, 2012.
24. Peter, M., Crapo, T., Gilbert, W., and Badylak, S.F. An overview of tissue and whole organ decellularization processes. Biomaterials **32,** 3233, 2011.
25. Kang, K.N., Kim, D.Y., Yoon, S.M., Kwon, J.S., Seo, H.W., Kim, E.S., Lee, B., Kim, J.H., Min, B.H., Lee, H.B., and Kim, M.S. In vivo release of bovine serum albumin from an injectable small intestinal submucosa gel. Int J Pharm **420,** 266, 2011.
26. Kim, K.S., Lee, J.Y., Kang, Y.M., Kim, E.S., Kim, G.H., Rhee, S.D., Cheon, H.G., Kim, J.H., Min, B.H., Lee, H.B., and Kim, M.S. Small intestine submucosa sponge for in vivo support of tissue-engineered bone formation in the presence of rat bone marrow stem cells. Biomaterials **31,** 1104, 2010.
27. Ahn, H.H., Kim, K.S., Lee, J.H., Lee, M.S., Song, I.B., Cho, M.H., Shin, N.Y., Khang, G., Lee, H.B., and Kim, M.S. Porcine small intestinal submucosa sheets as a scaffold for human bone marrow stem cells. Int J Biol Macromol **41,** 590, 2007.
28. Kim, M.S., Ahn, H.H., Cho, M.H., Shin, Y.N., Khang, G., and Lee, H.B. Porcine small intestinal submucosa sheets as a scaffold for human bone marrow stem cells. Biomaterials **28,** 5137, 2007.
29. Lee, M.S., Song, I.B., Khang, G., Kim, M.S., and Lee, H.B. Preparation and characterization of small intestinal submucosa coated with Alginate/Gelatin as a wound dressing. Key Eng Mater **342,** 69, 2007.
30. Kim, M.S., Lee, S.J., Lee, H.B., Shin, H.W., Kim, S.H., and Khang, G. Preparation of sponge using porcine small intestinal submucosa and their applications as a scaffold and a wound dressing. Adv Exp Med Biol **585,** 209, 2006.
31. Smith, R.M., Wiedl, C., Chubb, P., and Greene, C.H. Role of small intestine submucosa (SIS) as a nerve conduit: preliminary report. J Invest Surg **17,** 339, 2004.
32. Xei, X., Zhang, C., and Su, Y. Comparison between effects of small intestinal submucosa graft and inside-out vein graft on repairing peripheral nerve defects. Zhongguo Xiu Fu Chong Jian Wai Ke Za Zhi **21,** 149, 2007.
33. Hutmacher, D.W., and Cool, S. Concepts of scaffold-based tissue engineering-the rationale to use solid free-form fabrication techniques. J Cell Mol Med **11,** 654, 2007.
34. Hollister, S.J. Porous scaffold design for tissue engineering. Nat Mater **4,** 518, 2005.
35. Park, S.A., Lee, S.H., Kim, W.D., Han, I.H., and Park, J.C. Effect of plasma treatment on scaffold by solid freeform fabrication. Tissue Eng Reg Med **8,** 23, 2011.
36. Greca, F.H., de Noronha, L., Rodrigo, F., Marcolini, N., Verona, A., Pereira, I.A., and Bier, R.S. Small intestinal submucosa as a graft to increase rectum diameter. J Surg Res **183,** 503, 2013.
37. Jin, J., Limburg, S., Joshi, S.K., Landman, R., Park, M., Zhang, Q., Kim, H.T., and Kuo, A.C. Peripheral nerve repair in rats using composite hydrogel-filled aligned nanofiber conduits with incorporated nerve growth factor. Tissue Eng Part A **19,** 2138, 2013.
38. Andrée, B., Bär, A., Haverich, A., and Hilfiker, A. Small intestinal submucosa segments as matrix for tissue engineering: review. Tissue Eng Part B **19,** 279, 2013.
39. Kwon, D.Y., Kwon, J.S., Shim, S.W., Park, J.H., Lee, J.H., Kim, J.H., Kim, W.D., and Kim, M.S. Preparation of three-dimensional scaffolds by using solid freeform fabrication and feasibility study of the scaffolds. J Mater Chem B **2,** 1698, 2014.
40. Tang, S., Zhu, J., Xu, Y., Xiang, A.P., Jiang, M.H., and Quan, D. The effects of gradients of nerve growth factor immobilized PCLA scaffolds on neurite outgrowth in vitro and peripheral nerve regeneration in rats. Biomaterials **34,** 7086, 2013.
41. Kim, J.R., Oh, S.H., Kwon, G.B., Namgung, U.K., Song, K.S., Jeon, B.H., and Lee, J.H. Acceleration of peripheral nerve regeneration through asymmetrically porous nerve guide conduit applied with biological/physical stimulation. Tissue Eng Part A **19,** 2674, 2013.
42. Niu, Y., Chen, K.C., He, T., Yu, W., Huang, S., and Xu, K. Scaffolds from block polyurethanes based on poly(ε-caprolactone) (PCL) and poly(ethylene glycol) (PEG) for peripheral nerve regeneration. Biomaterials **35,** 4266, 2014.
43. Ohtsubo, S., Ishikawa, M., Kamei, N., Kijima, Y., Suzuki, O., Sunagawa, T., Higashi, Y., Masuda, H., Asahara, T., and Ochi, M. The therapeutic potential of ex vivo expanded CD133+ cells derived from human peripheral blood for peripheral nerve injuries. J Neurosurg **117,** 787, 2012.
44. Hailang, L., Bin, Z., Yongjie, Z., and Yan, J. Tissue-engineered nerve constructs under a microgravity system for peripheral nerve regeneration. Tissue Eng Part A 2014 [Epub ahead of print]; DOI:10.1089/ten.tea.2013.0565.
45. Ikeda, M., Uemura, T., Takamatsu, K., Okada, M., Kazuki, K., Tabata, Y., Ikada, Y., and Nakamura, H. Acceleration of peripheral nerve regeneration using nerve conduits in combination with induced pluripotent stem cell technology and a basic fibroblast growth factor drug delivery system. J Biomed Mater Res A **102,** 1370, 2013.
46. Kaemmer, D., Bozkurt, A., Otto, J., Junge, K., Klink, C., Weis, J., Sellhaus, B., O'Dey, D.M., Pallua, N., Jansen, M., Schumpelick, V., and Klinge, U. Evaluation of tissue components in the peripheral nervous system using Sirius red staining and immunohistochemistry: a comparative study (human, pig, rat). J Neurosci Methods **190,** 112, 2010.

Address correspondence to:
Moon Suk Kim, PhD
Department of Molecular Science and Technology
Ajou University
Suwon 443-749
Korea

E-mail: moonskim@ajou.ac.kr

Received: March 19, 2014
Accepted: October 30, 2014
Online Publication Date: January 7, 2015